SUPPORTING INFORMATION

Pinofuranoxins A and B, Bioactive Tetrasubstituted Furanones Produced by the Invasive Pathogen *Diplodia sapinea*

Marco Masi,[†] Roberta Di Lecce,[†] Giulia Marsico,[‡] Benedetto Teodoro Lunaldeddu,[±] Lucia Maddau,[§] Stefano Superchi,[‡] and Antonio Evidente*,[†]

[†]Dipartimento di Scienze Chimiche, Università di Napoli Federico II, Complesso Universitario Monte Sant'Angelo, Via Cintia 4, 80126, Napoli, Italy

[‡]Dipartimento di Scienze, Università della Basilicata, Viale dell'Ateneo Lucano 10, 85100 Potenza, Italy.

[±]Dipartimento Territorio e Sistemi Agro-Forestali, Università di Padova, Viale dell'Università 16, Legnaro 35020, Italy

[§]Dipartimento di Agraria, Sezione di Patologia Vegetale ed Entomologia, Università degli Studi di Sassari, Viale Italia 39, 07100, Sassari, Italy

Supporting Information List

Table S1. NOESY Data of Pinofuranoxins A and B (1 and 2)

1		**2**	
Irradiated	Observed	Irradiated	Observed
H-4	Me-10	H-4	Me-10
H-5	Me-10	H-5	Me-10
H-8	Me-9	H-7	H-8
		H-8	Me-9

Table S2. Conformers Boltzmann distribution of (4*S*,5*R*,7*R*,8*R*)-**1a**.

DFT/B3LYP/6-311++G(2d,2p)/(IEFPCM(CH_3CN)

Conformers	ΔG (Kcal/mol)	% Pop
C1	0.000000	39.3
C2	0.212553	27.4
C3	0.491568	17.1
C4	0.526053	16.2

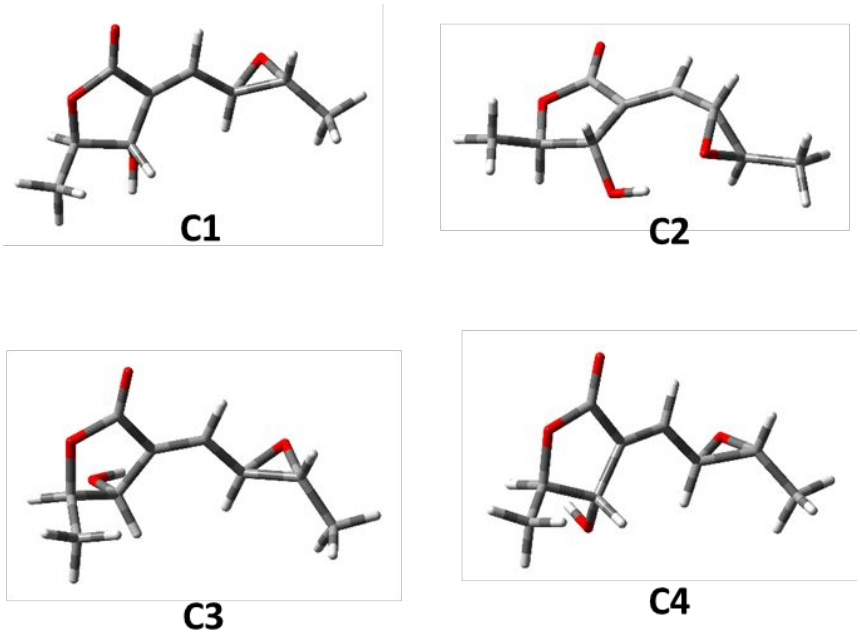

Figure S1. Minimum energy conformers of (4*S*,5*R*,7*R*,8*R*)-**1a** computed at DFT/B3LYP/6-311++G(2d,2p)/IEFPCM(CH_3CN) level. Conformers C2 displays intramolecular H-bond.

Table S3. Conformers Boltzmann distribution of (4*S*,5*R*,7*S*,8*S*)-**1b**.
DFT/B3LYP/6-311++G(2d,2p))/(IEFPCM(CH_3CN)

Conformers	ΔG (Kcal/mol)	% Pop
C1	0.000000	41.4
C2	0.299079	25.0
C3	0.493449	18.0
C4	0.581229	15.5

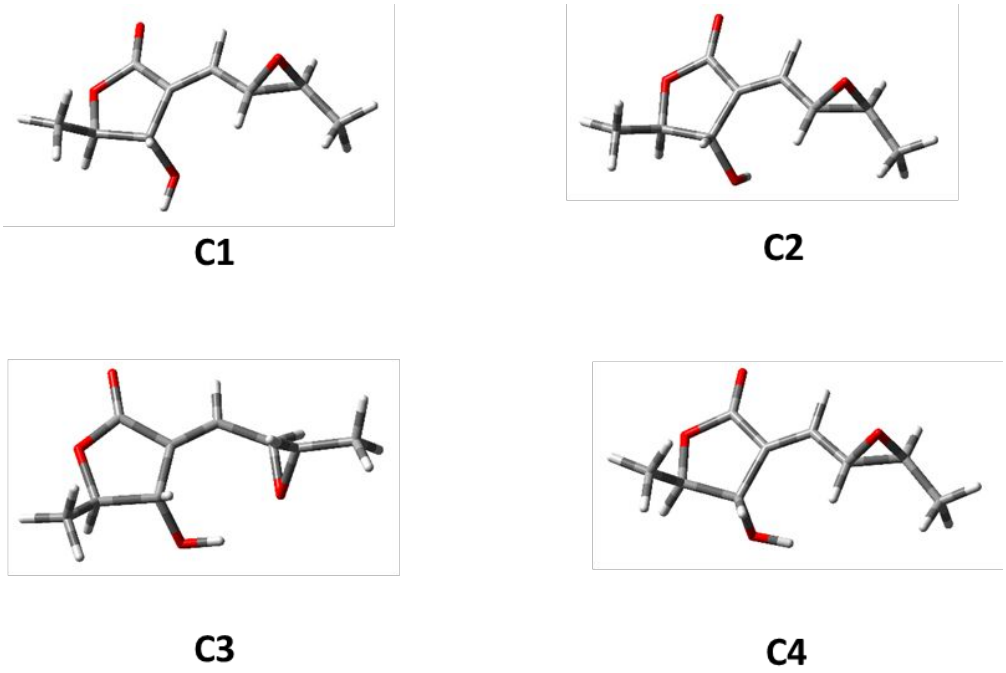

Figure S2. Minimum energy conformers of (4*S*,5*R*,7*S*,8*S*)-**1b** computed at DFT/B3LYP/6-311++G(2d,2p)/IEFPCM(CH_3CN) level. Conformers C3 displays intramolecular H-bond.

Table S4. Conformers Boltzmann distribution of (4*S*,5*R*,7*R*,8*S*)-**2a**.

DFT/B3LYP/6-311++G(2d,2p))/(IEFPCM(CH_3CN)

Conformers	ΔG (Kcal/mol)	% Pop
C1	0.000000	59.9
C2	0.795663	15.6
C3	0.800679	15.5
C4	1.131108	8.9

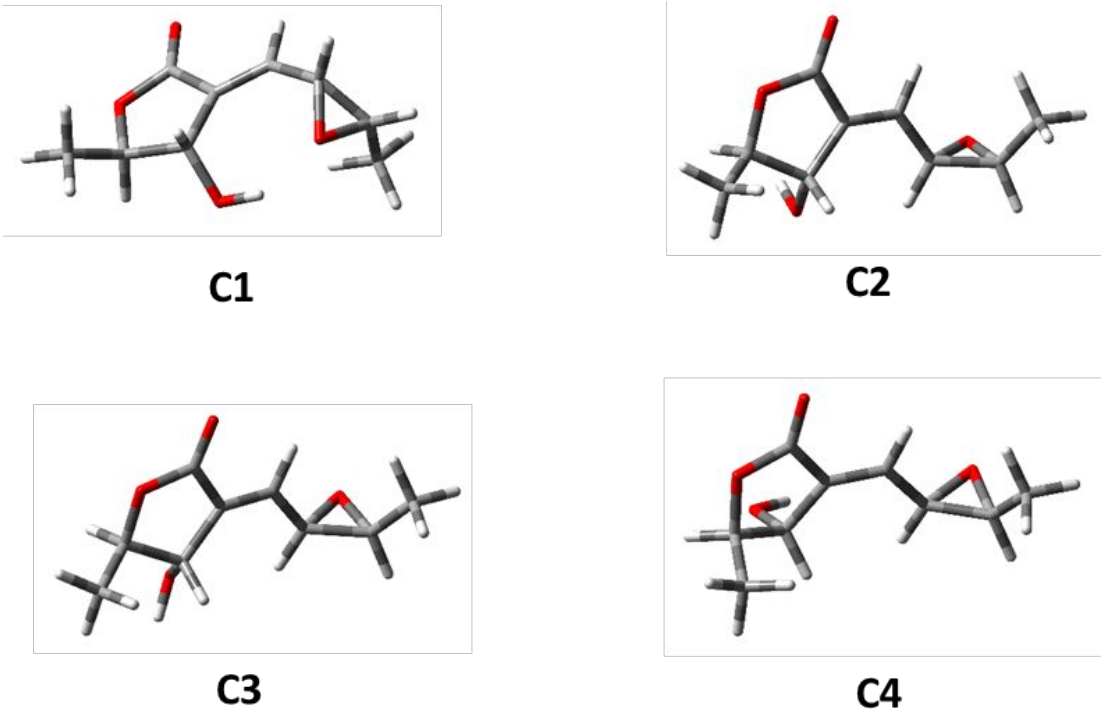

Figure S3. Structures of conformers found of (4*S*,5*R*,7*R*,8*S*)-**2a** computed at DFT/B3LYP/6-311++G(2d,2p)/IEFPCM(CH_3CN) level. Conformers C1 displays intramolecular H-bond.

Table S5. Conformers Boltzmann distribution of (4*S*,5*R*,7*S*,8*R*)-**2b**.
DFT/B3LYP/6-311++G(2d,2p))/(IEFPCM(CH_3CN)

Conformers	ΔG (Kcal/mol)	% Pop
C1	0.000000	35.8
C2	0.282777	22.2
C3	0.426360	17.4
C4	0.537339	14.4
C5	0.741741	10.2

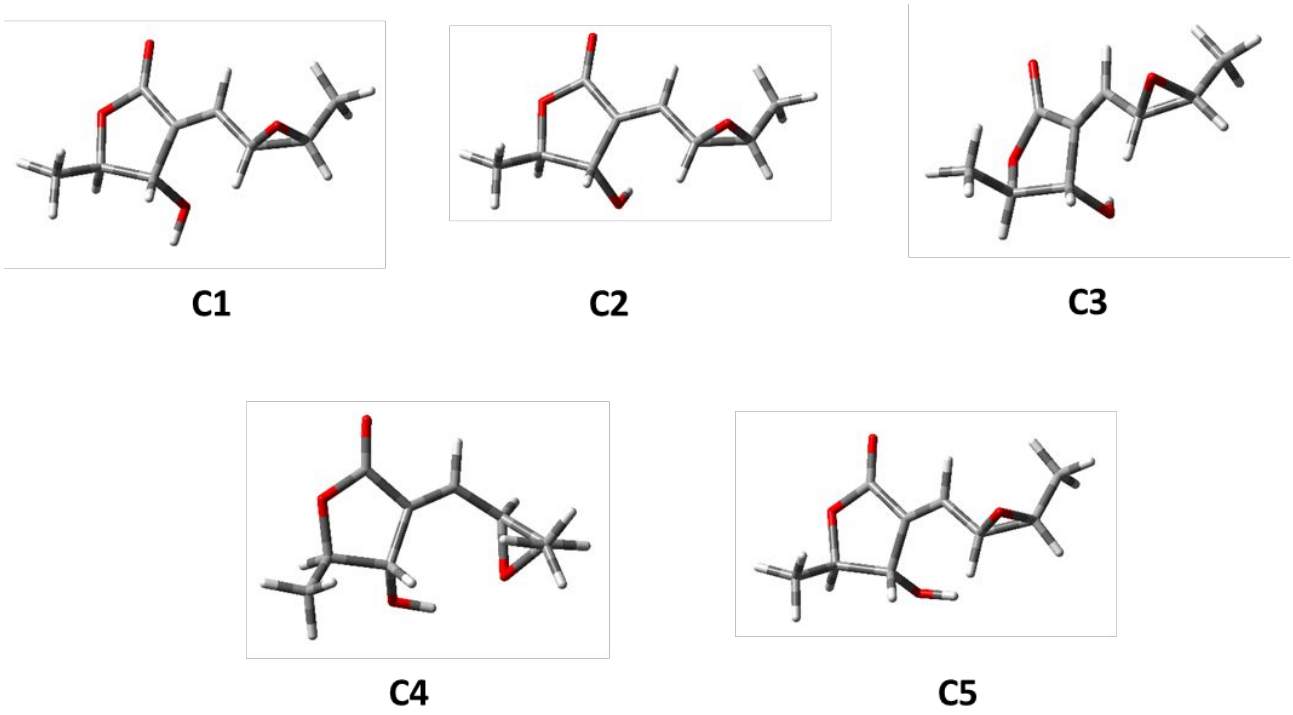

Figure S4. Structures of conformers found of (4*S*,5*R*,7*S*,8*R*)-**2b** computed at DFT/B3LYP/6-311++G(2d,2p)/IEFPCM(CH_3CN) level. Conformers C4 displays intramolecular H-bond.

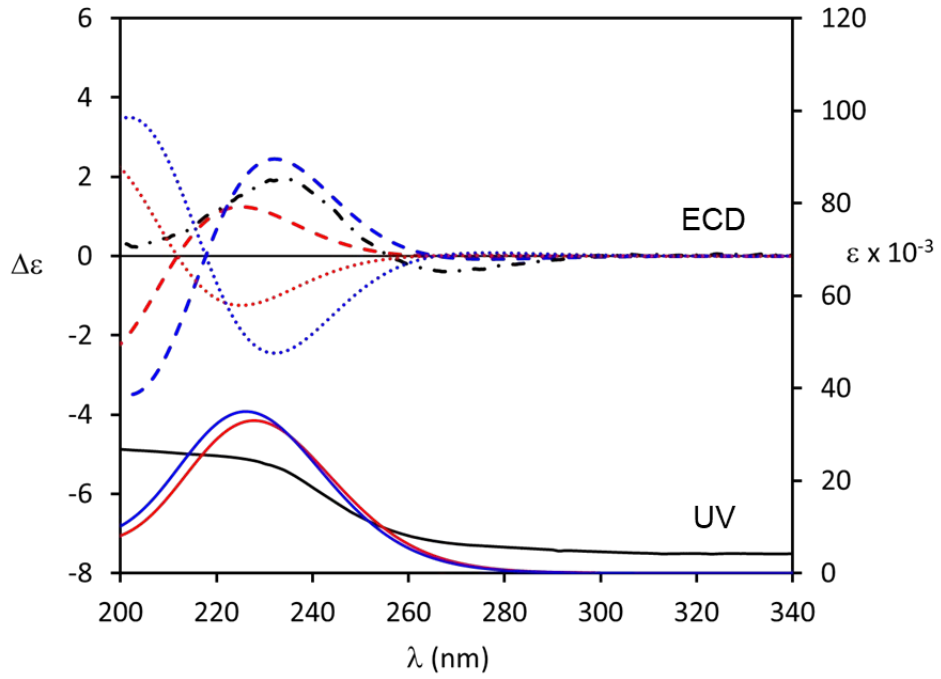

Figure S5. Comparison between experimental UV (solid black lines) and ECD spectra (dashed-dotted black line) of (+)-**1** with calculated [TDDFT/CAM-B3LYP/aug-cc-pVDZ/IEFPCM(CH_3CN)] ones. Computed UV spectrum for **1a** (solid red line) and **1b** (solid blue line). Computed ECD spectrum for (4*S*,5*R*,7*R*,8*R*)-**1a** (dotted red line), (4*R*,5*S*,7*S*,8*S*)-**ent-1a** (dashed red line), (4*S*,5*R*,7*S*,8*S*)-**1b** (dotted blue line), and (4*R*,5*S*,7*R*,8*R*)-**ent-1b** (dashed blue line). The calculated ECD spectra were divided by 2.

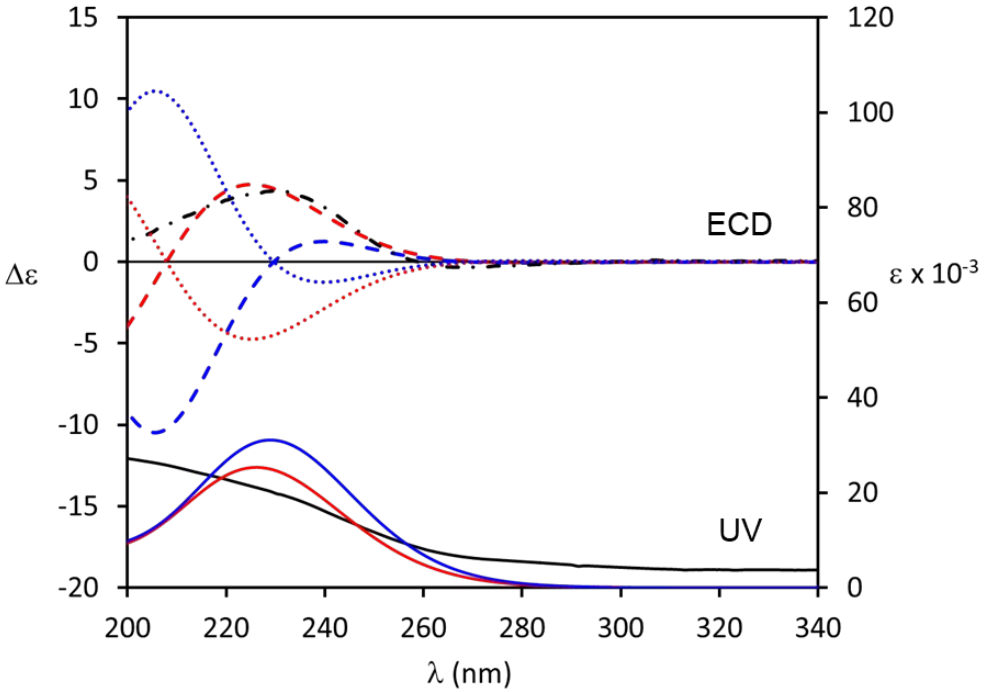

Figure S6. Comparison between experimental UV (solid black lines) and ECD (dashed-dotted black line) spectra of (+)-**2** with calculated [TDDFT/CAM-B3LYP/aug-cc-pVDZ/IEFPCM(CH_3CN)] ones. Computed UV spectrum for **2a** (solid red line) and **2b** (solid blue line). Computed ECD spectrum for (4*S*,5*R*,7*R*,8*S*)-**2a** (dotted red line), (4*R*,5*S*,7*S*,8*R*)-**ent-2a** (dashed red line), (4*S*,5*R*,7*S*,8*R*)-**2b** (dotted blue line), and (4*R*,5*S*,7*R*,8*S*)-**ent-2b** (dashed blue line).

ECD computations with explicit solvent model.

To further confirm the absolute configuration assignment the ECD spectra were also carried out ECD computations by simulating the solvent effects in an explicit approach. In fact, it is known that even with the weak hydrogen bond accepting solvent acetonitrile a better description of the solvent-solute interaction is often obtained by performing computations in the explicit solvent mode, i.e. including one or more solvent molecules in the input structures. Computational conformational analysis was then repeated at DFT/B3LYP/6-311++G(2d,2p) level of theory, adding a single molecule of acetonitrile H-bonded to the OH moiety of (4*S*,5*R*,7*R*,8*R*)-**1a** and (4*S*,5*R*,7*S*,8*S*)-**1b**. Four populated conformers were obtained for both diastereomers (see Table S5, Figure S7, Table S6, and Figure S8). Those displaying intramolecular H-bonding were again discarded and UV and ECD spectra were computed at TDDFT/CAM-B3LYP/aug-cc-pVDZ level on the remaining structures. Comparison of the UV and ECD spectra computed in the explicit solvent mode with the experimental spectra (Figure S9) supports the above assignment of (4*R*,5*S*,7*R*,8*R*) AC to pinofuranoxin A (+)-(**1**). The same analysis, employing the explicit solvent approach, has been performed also for pinofuranoxin B (**2**). For this compound four populated conformers were obtained for both diastereomers (4*S*,5*R*,7*R*,8*S*)-**2a** and (4*S*,5*R*,7*S*,8*R*)-**2b** (see Table S7, Figure S10, Table S8, and Figure S11). Those displaying intramolecular H-bonding were again discarded and UV and ECD spectra were computed on the remaining structures. Comparison of the UV and ECD spectra computed in the explicit solvent mode with the experimental spectra (Figure S12) supports the above assignment of (4*R*,5*S*,7*S*,8*R*) AC to pinofuranoxin B (+)-(**2**).

Table S6. Conformers Boltzmann distribution of (4*S*,5*R*,7*R*,8*R*)-**1a·ACN** adduct.
DFT/B3LYP/6-311++G(2d,2p)

Conformers	ΔG (Kcal/mol)	% Pop
C1	0.000000	67.0
C2	0.674652	21.5
C3	1.302279	7.4
C4	1.654026	4.1

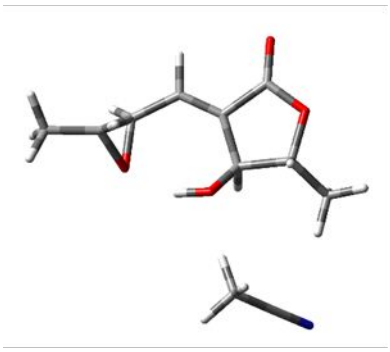

C1

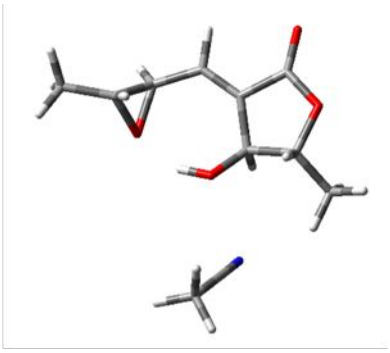

C2

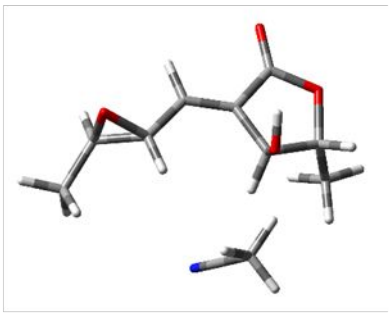

C3

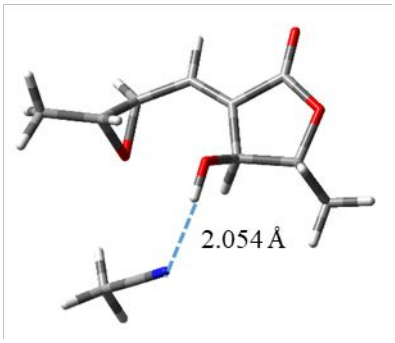

C4

Figure S7. Structures of most stable conformers of (4*S*,5*R*,7*R*,8*R*)-**1a·ACN** adduct calculated at DFT/B3LYP/6-311++G(2d,2p) level of theory. Conformers C1 and C2 display intramolecular H-bond, while conformer C4 intermolecular H-bond with acetonitrile.

Table S7. Conformers Boltzmann distribution of (4*S*,5*R*,7*S*,8*S*)-**1b**·**ACN** adduct.
DFT/B3LYP/6-311++G(2d,2p)

Conformers	ΔG (Kcal/mol)	% Pop
C1	0.000000	78.0
C2	1.183149	10.6
C3	1.350558	8.0
C4	1.854039	3.4

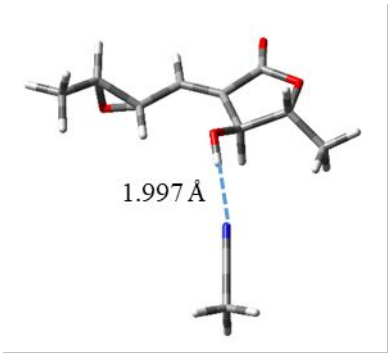

C1

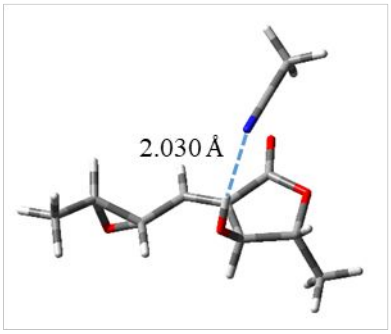

C2

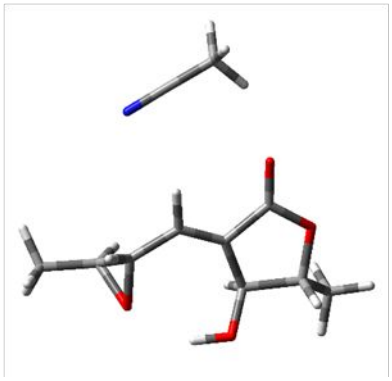

C3

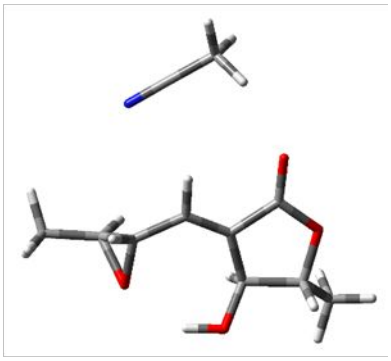

C4

Figure S8. Structures of most stable conformers of (4*S*,5*R*,7*S*,8*S*)-**1b**·**ACN** adduct calculated at DFT/B3LYP/6-311++G(2d,2p) level of theory. Conformers C3 and C4 display intramolecular H-bond, while conformers C1 and C2 intermolecular H-bond with acetonitrile.

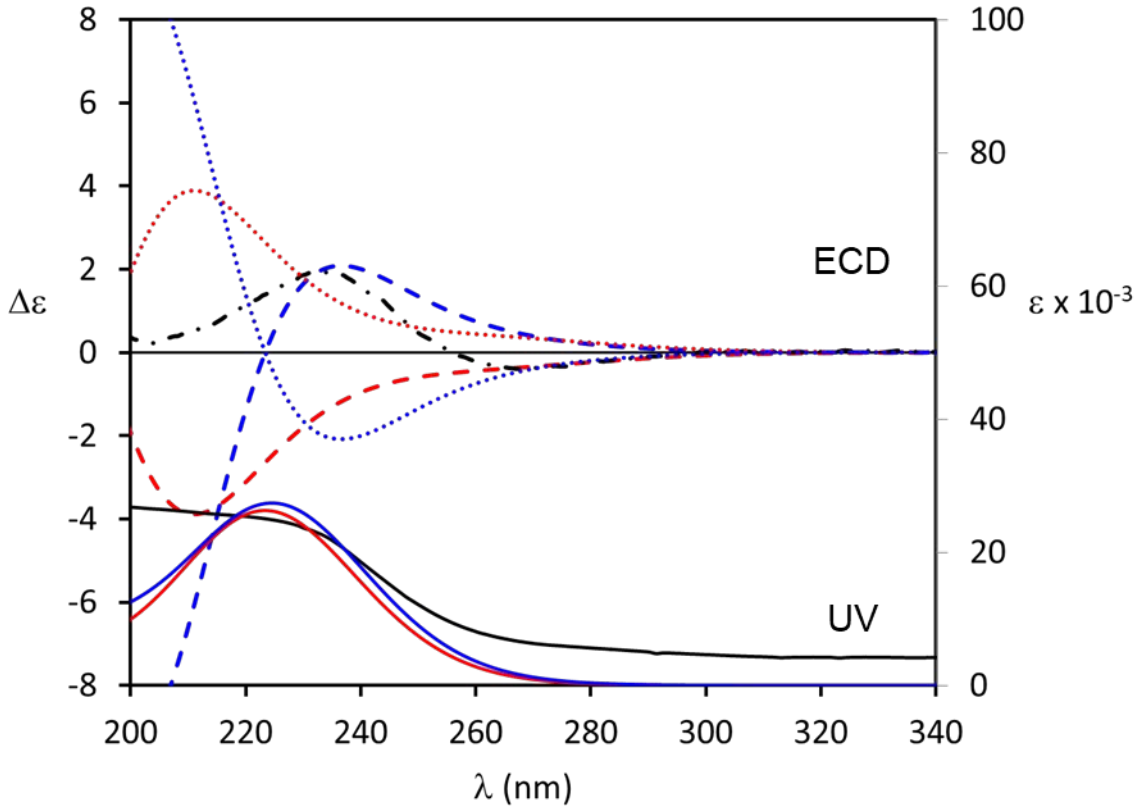

Figure S9. Comparison between experimental UV (solid black lines) and ECD (dashed-dotted black line) spectra of (+)-**1** with calculated [TDDFT/CAM-B3LYP/aug-cc-pVDZ/explicit model(CH_3CN)] ones. Computed UV spectrum for **1a·ACN** adduct (solid red line) and **1b·ACN** adduct (solid blue line). Computed ECD spectrum for (4*S*,5*R*,7*R*,8*R*)-**1a·ACN** adduct (dotted red line), (4*R*,5*S*,7*S*,8*S*)-**ent-1a·ACN** adduct (dashed red line), (4*S*,5*R*,7*S*,8*S*)-**1b·ACN** adduct (dotted blue line), and (4*R*,5*S*,7*R*,8*R*)-**ent-1b·ACN** adduct (dashed blue line). The calculated ECD spectra were divided by 2. Conformers with intramolecular hydrogen bonding have been removed (see text).

Table S8. Conformers Boltzmann distribution of (4*S*,5*R*,7*R*,8*S*)-**2a**·**ACN** adduct.
DFT/B3LYP/6-311++G(2d,2p)

Conformers	ΔG (Kcal/mol)	% Pop
C1	0.000000	49.4
C2	0.231363	33.4
C3	0.675279	15.8
C4	2.109855	1.4

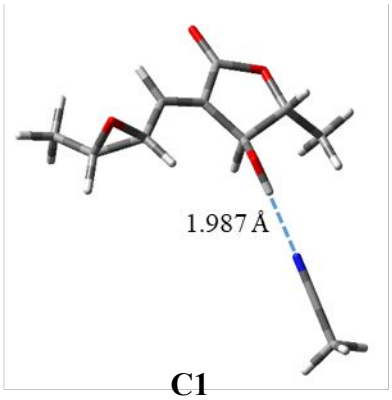

C1

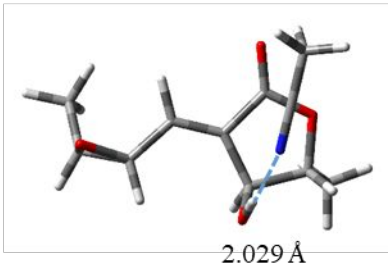

C2

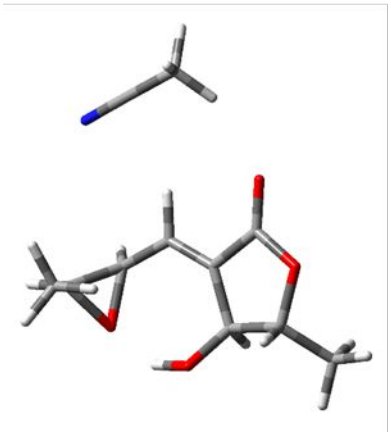

C3

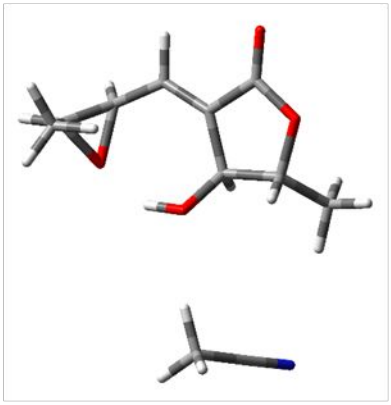

C4

Figure S10. Structures of most stable conformers of (4*S*,5*R*,7*R*,8*S*)-**2a**·**ACN** adduct calculated at DFT/B3LYP/6-311++G(2d,2p) level of theory. Conformers C3 and C4 display intramolecular H-bond, while conformers C1 and C2 intermolecular H-bond with acetonitrile.

Table S9. Conformers Boltzmann distribution of (4*S*,5*R*,7*S*,8*R*)-**2b·ACN** adduct.
DFT/B3LYP/6-311++G(2d,2p)

Conformers	ΔG (Kcal/mol)	% Pop
C1	0.000000	55.8
C2	0.158631	42.7
C3	2.576970	0.7
C4	2.594526	0.7

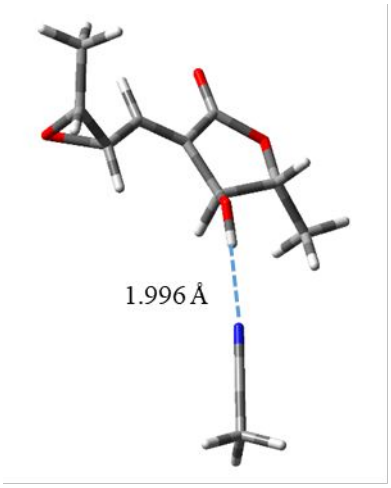

C1

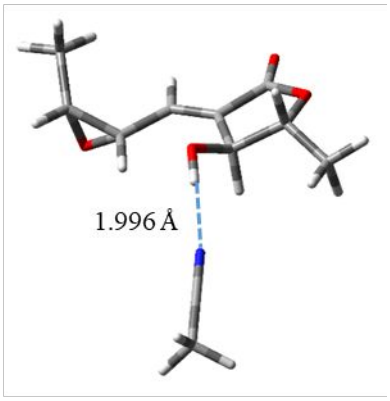

C2

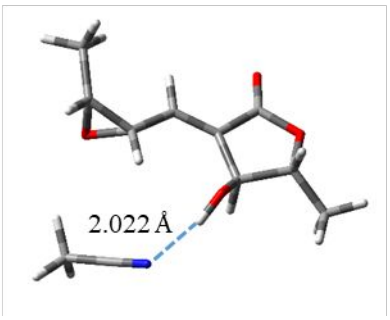

C3

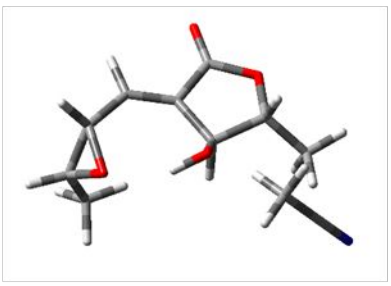

C4

Figure S11. Structures of most stable conformers (4*S*,5*R*,7*S*,8*R*)-**2b·ACN** adduct calculated at DFT/B3LYP/6-311++G(2d,2p) level of theory. Conformers displays intramolecular H-bond, while conformers C1, C2, and C3 intermolecular H-bond with acetonitrile.

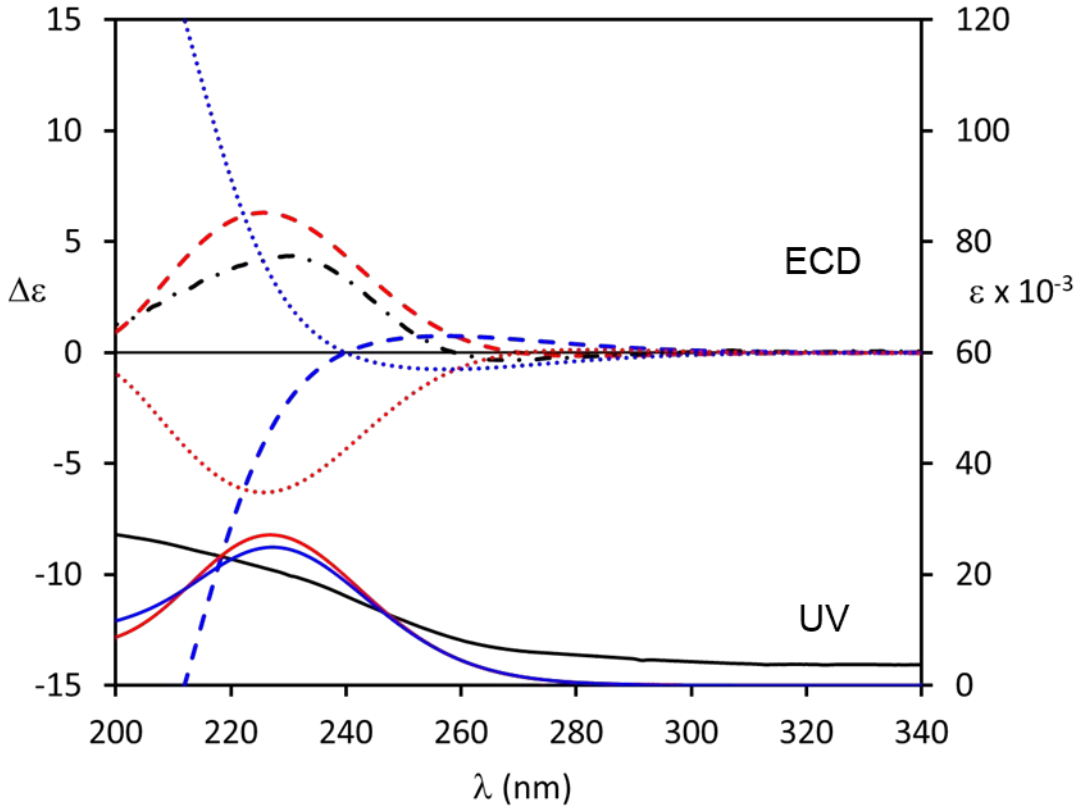

Figure S12. Comparison between experimental UV (solid black lines) and ECD (dashed-dotted black line) spectra of (+)-**2** with calculated [TDDFT/CAM-B3LYP/aug-cc-pVDZ/explicit model(CH_3CN)] ones. Computed UV spectrum for **2a·ACN** adduct (solid red line) and **2b·ACN** adduct (solid blue line). Computed ECD spectrum for (4*S*,5*R*,7*R*,8*S*)-**2a·ACN** adduct (dotted red line), (4*R*,5*S*,7*S*,8*R*)-**ent-2a·ACN** adduct (dashed red line), (4*S*,5*R*,7*S*,8*R*)-**2b·ACN** adduct (dotted blue line), and (4*R*,5*S*,7*R*,8*S*)-**ent-2b·ACN** adduct (dashed blue line). Conformers with intramolecular hydrogen bonding have been removed (see text).

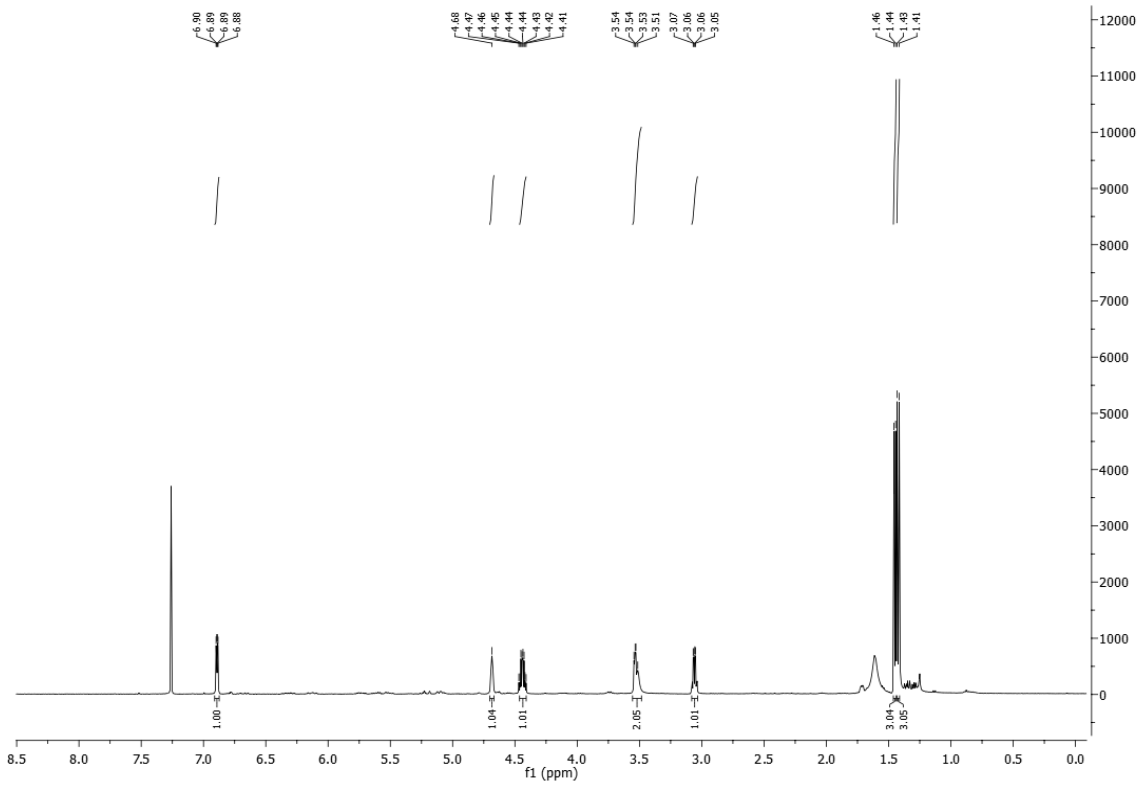

Spectrum 1. ^{1}H NMR spectrum of pinofuranoxin A (**1**) ($CDCl_3$, 400 MHz).

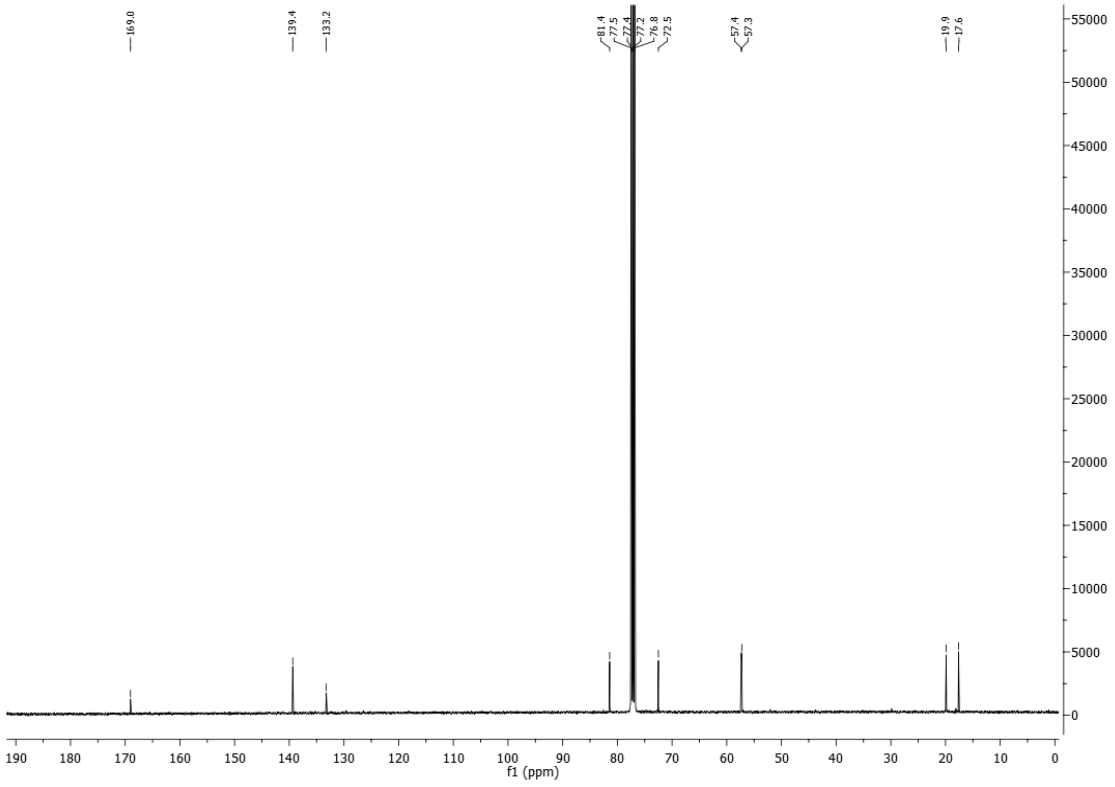

Spectrum 2. ^{13}C NMR spectrum of pinofuranoxin A (**1**) ($CDCl_3$, 100 MHz).

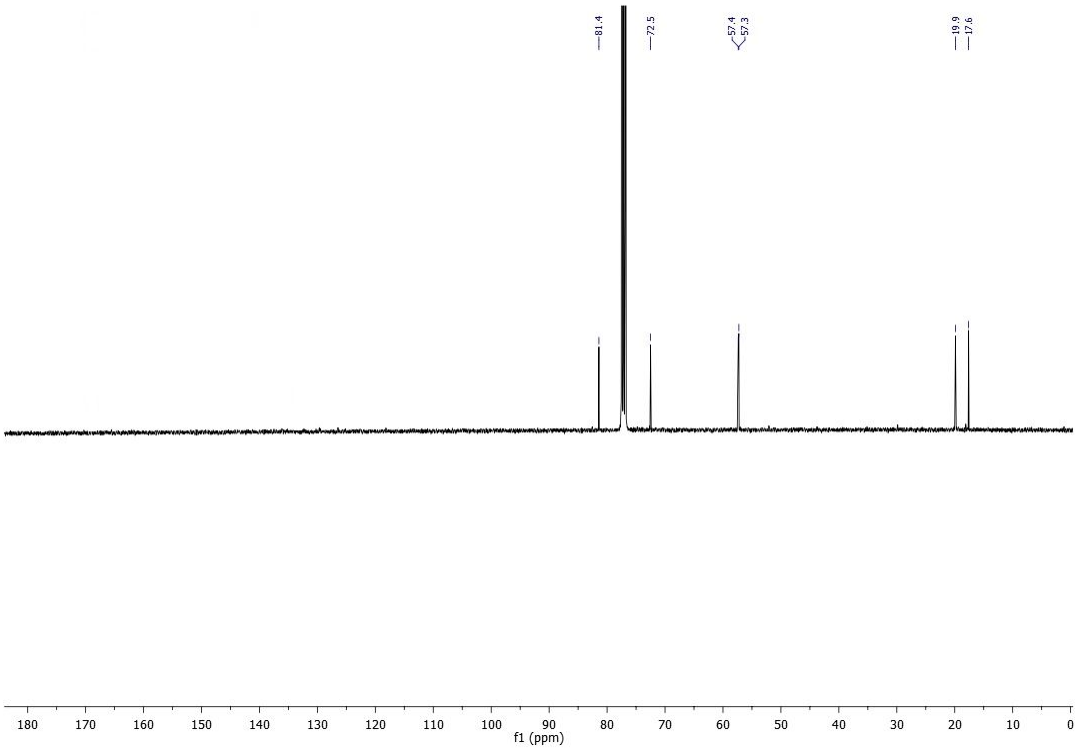

Spectrum 3. DEPT-135 NMR spectrum of pinofuranoxin A (**1**) ($CDCl_3$, 100 MHz).

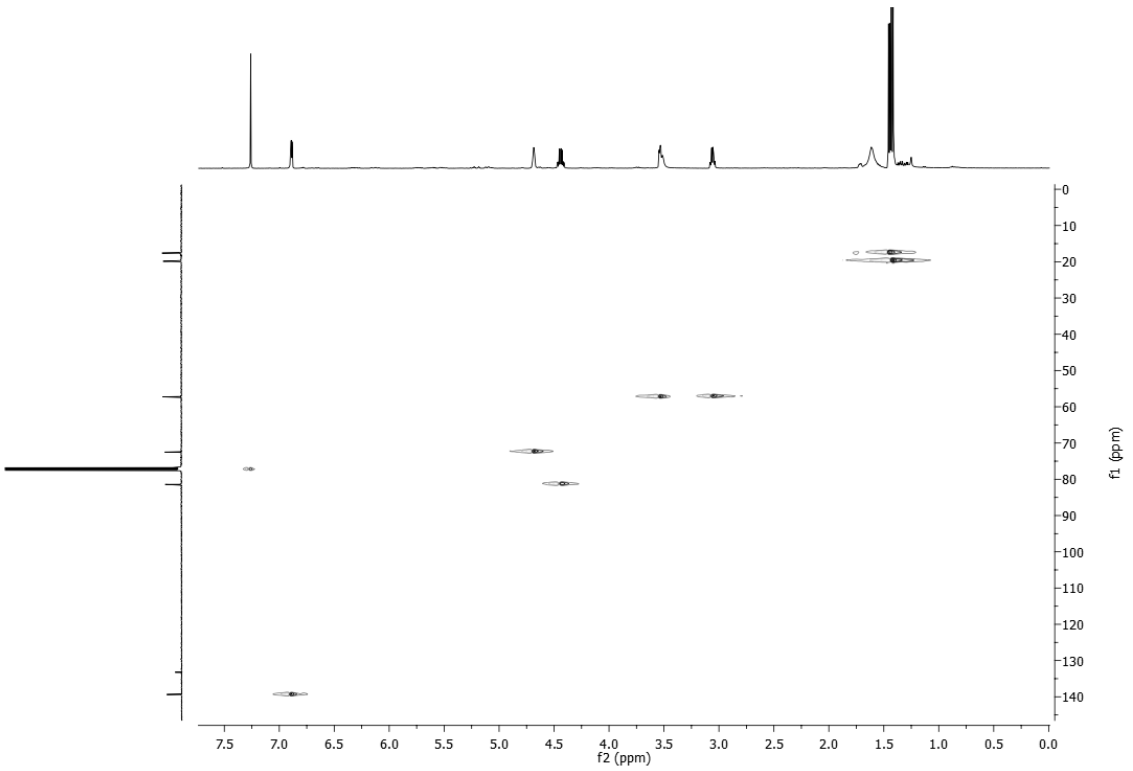

Spectrum 4. HSQC spectrum of pinofuranoxin A (**1**) ($CDCl_3$, 400/100 MHz).

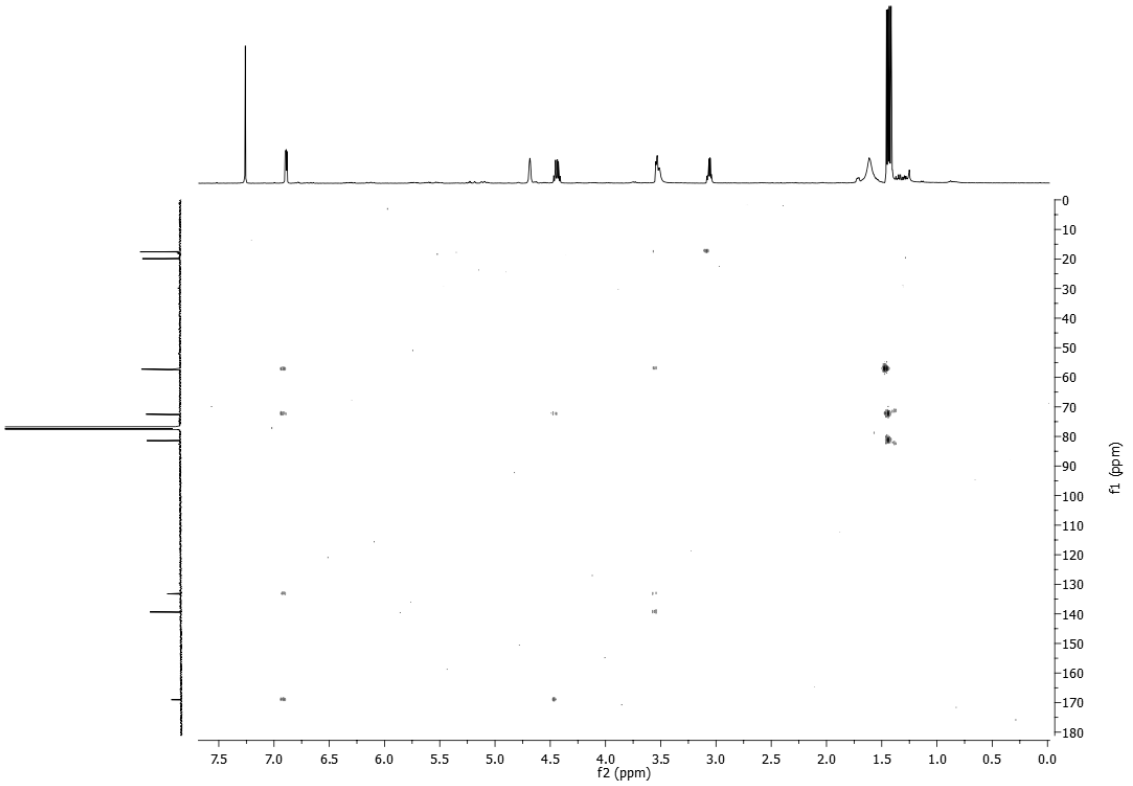

Spectrum 5. HMBC spectrum of pinofuranoxin A (**1**) ($CDCl_3$, 400/100 MHz).

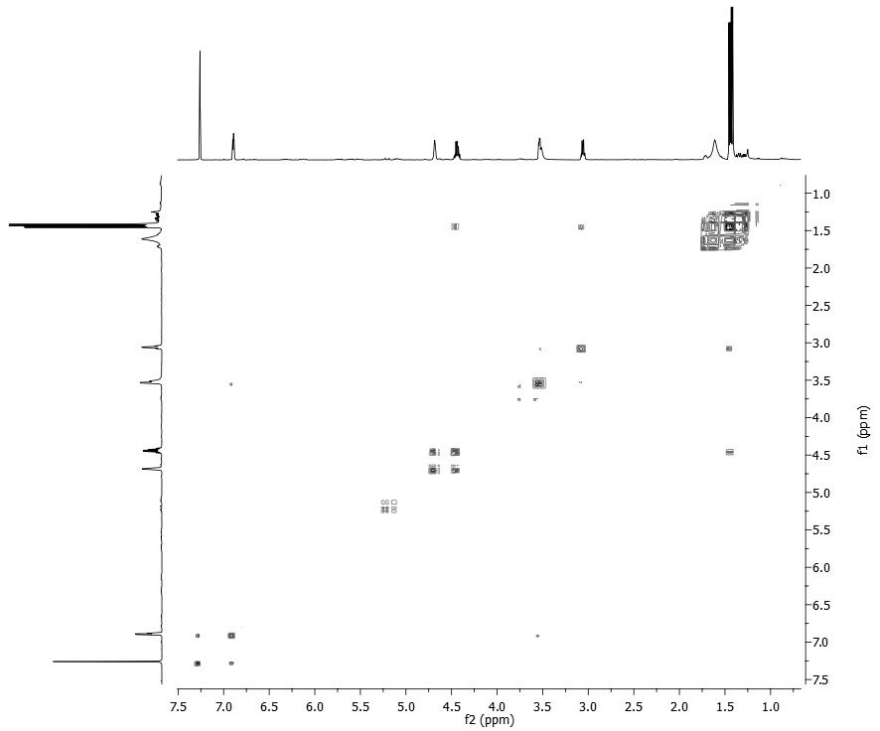

Spectrum 6. COSY spectrum of pinofuranoxin A (**1**) ($CDCl_3$, 400 MHz).

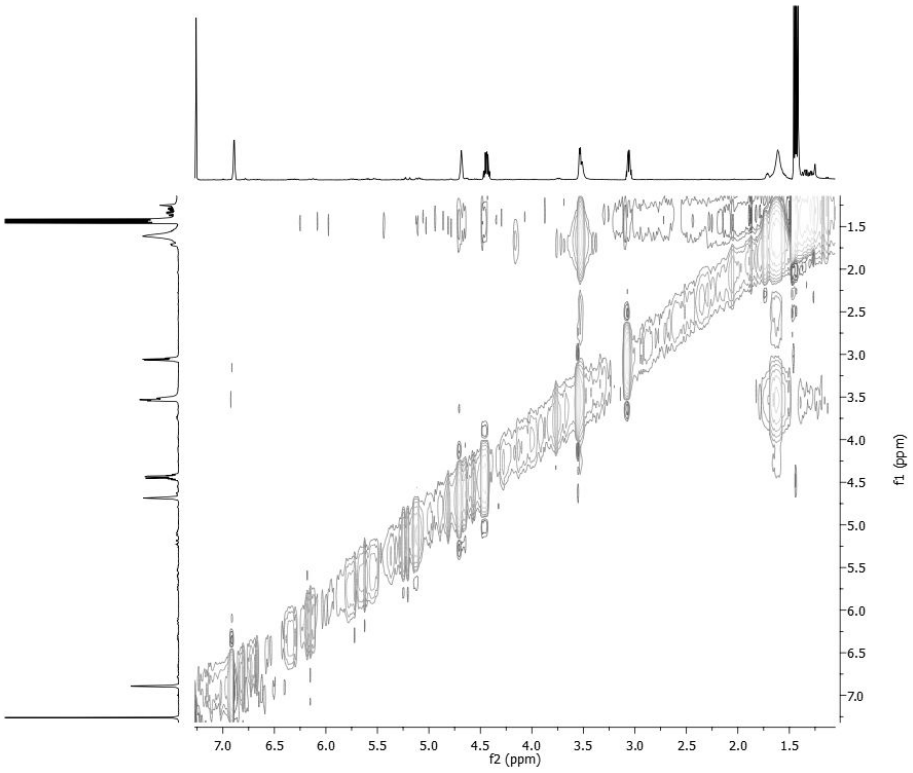

Spectrum 7. NOESY spectrum of pinofuranoxin A (**1**) ($CDCl_3$, 400 MHz).

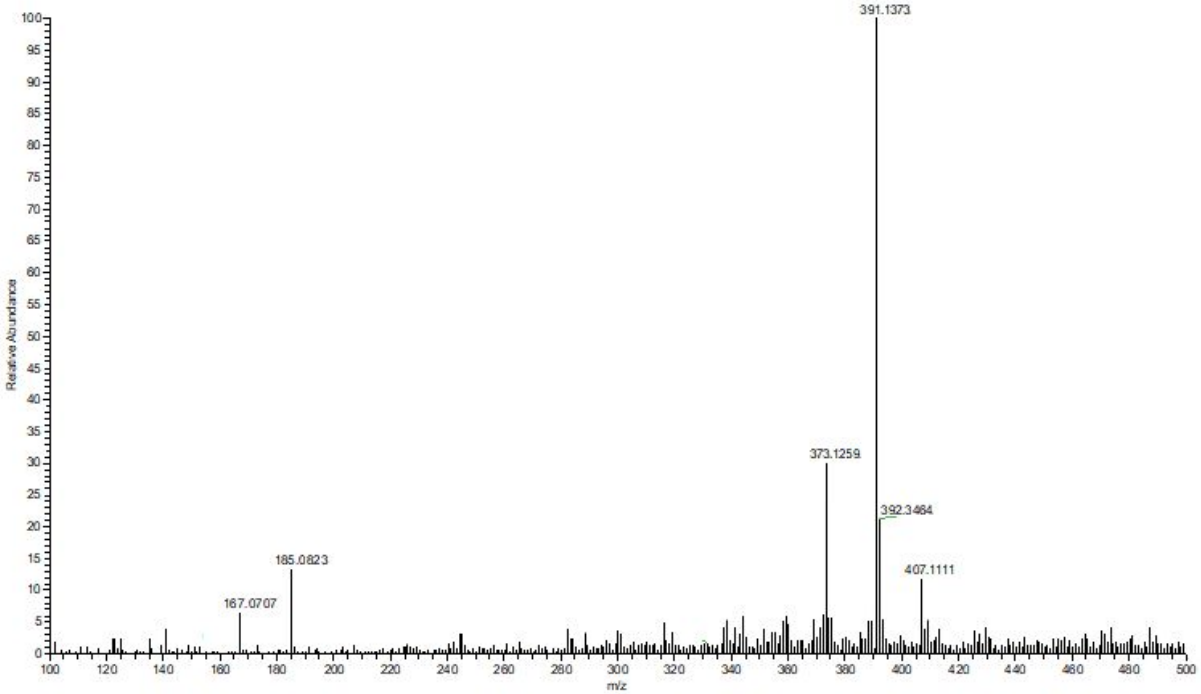

Spectrum 8. HR ESIMS spectrum of pinofuranoxin A (**1**).

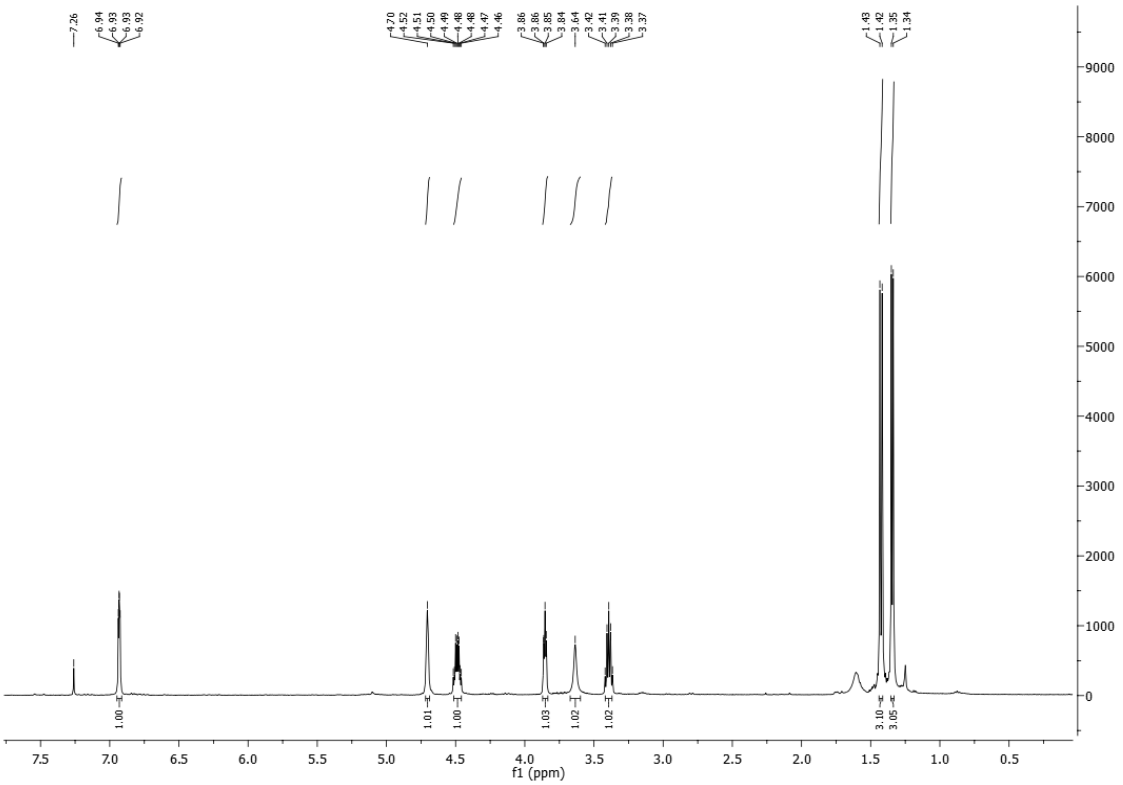

Spectrum 9. ^{1}H NMR spectrum of pinofuranoxin B (**2**) ($CDCl_3$, 400 MHz).

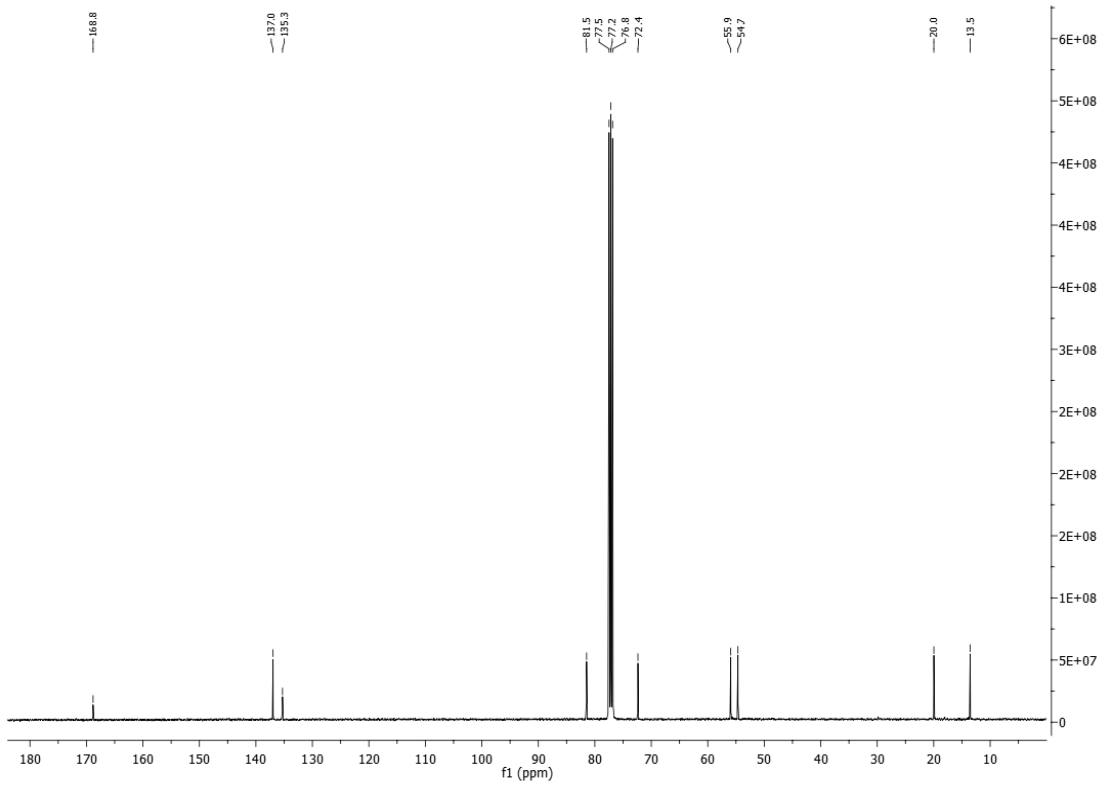

Spectrum 10. ^{13}C NMR spectrum of pinofuranoxin B (**2**) ($CDCl_3$, 100 MHz).

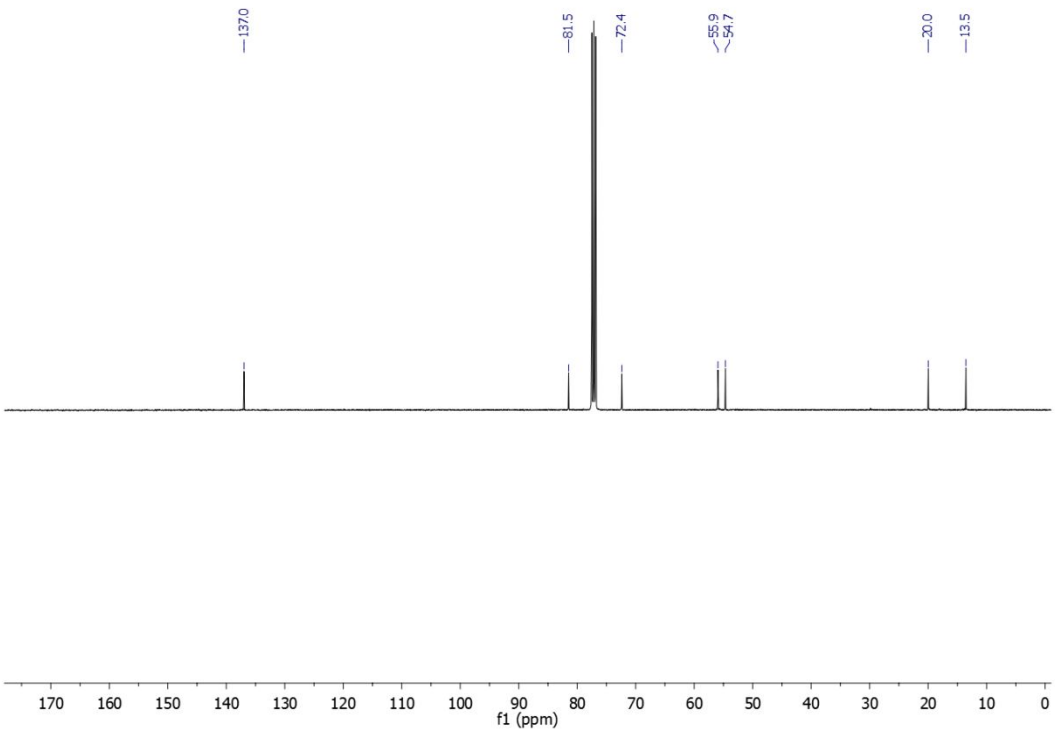

Spectrum 11. DEPT-135 NMR spectrum of pinofuranoxin B (**2**) ($CDCl_3$, 100 MHz).

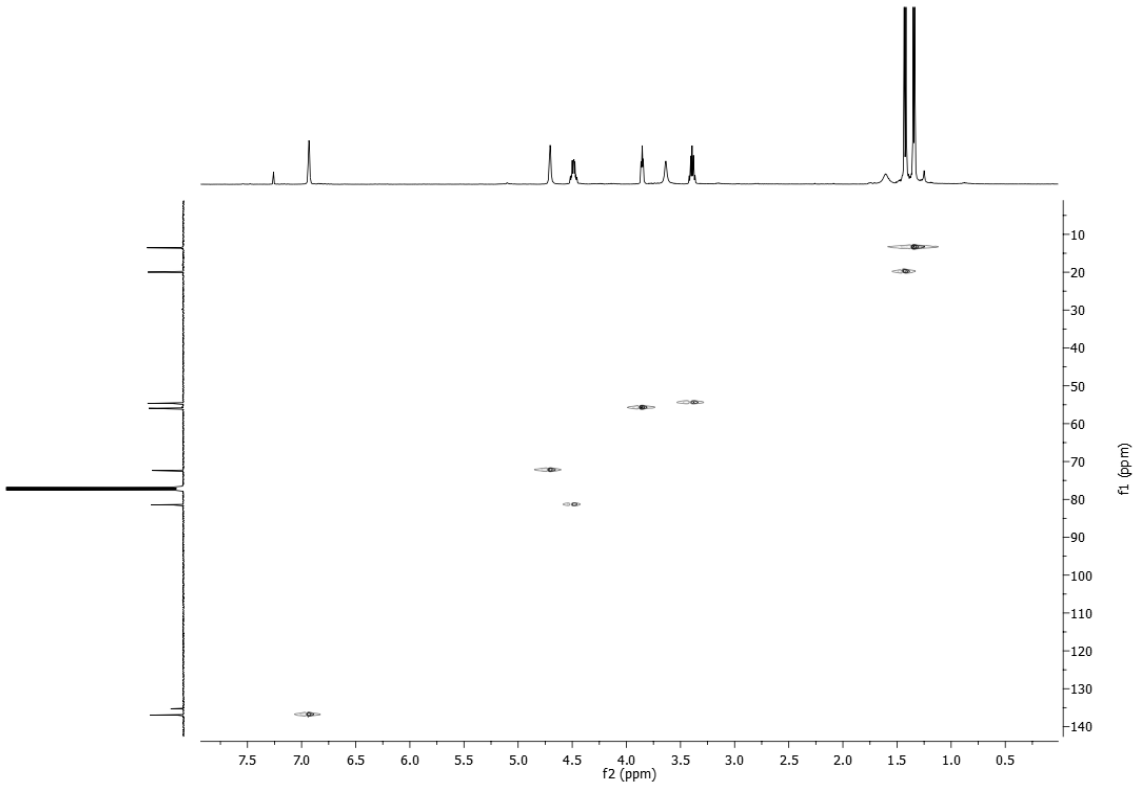

Spectrum 11. HSQC spectrum of pinofuranoxin B (**2**) ($CDCl_3$, 400/100 MHz).

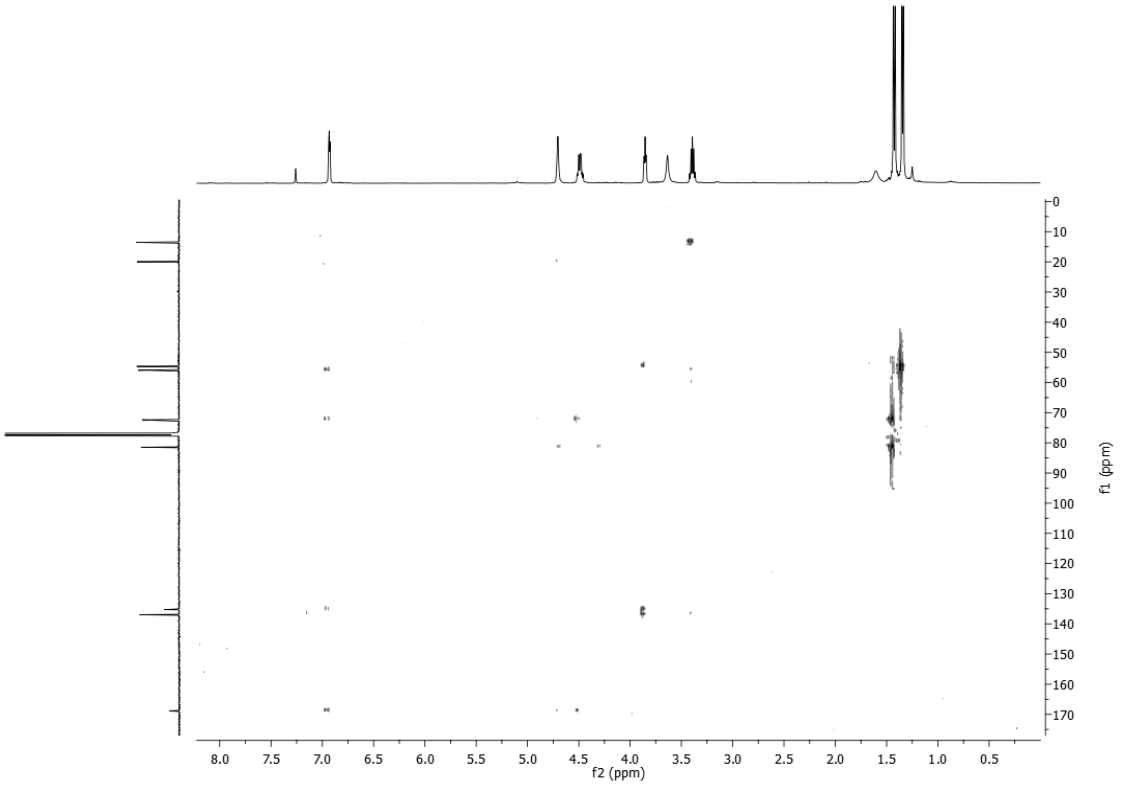

Spectrum 11. HMBC spectrum of pinofuranoxin B (**2**) ($CDCl_3$, 400/100 MHz).

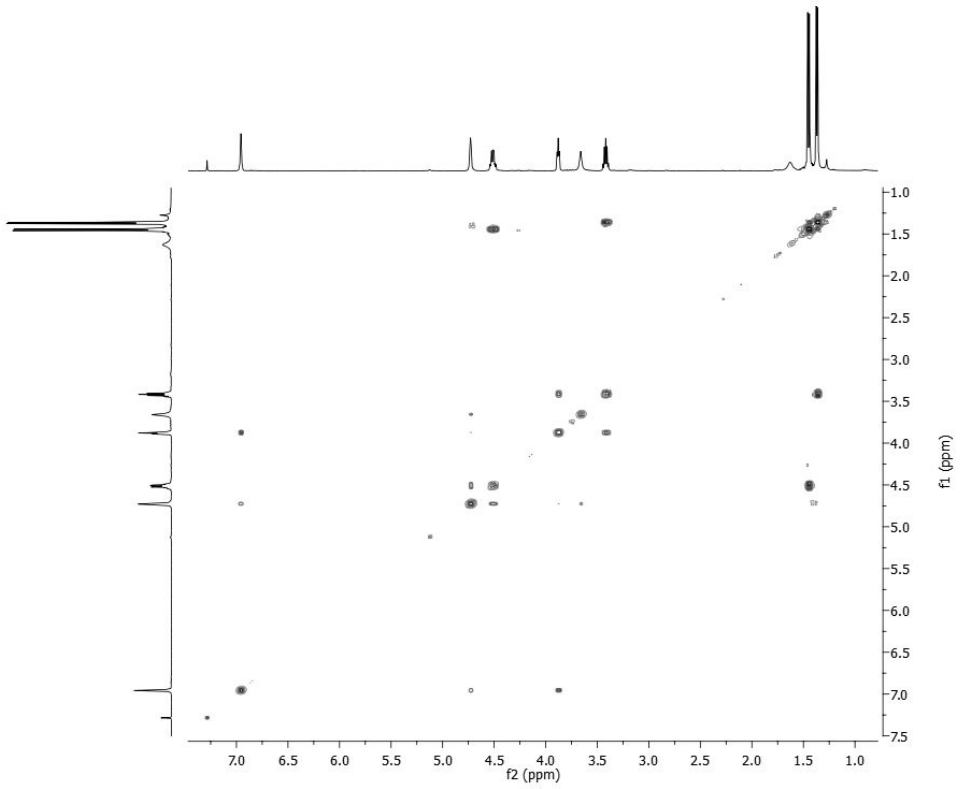

Spectrum 12. COSY spectrum of pinofuranoxin B (**2**) ($CDCl_3$, 400 MHz).

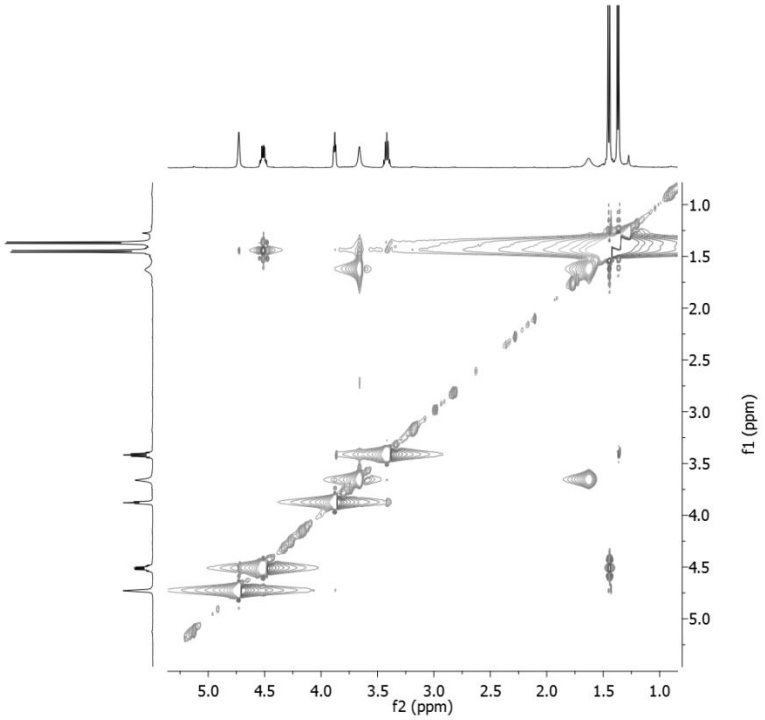

Spectrum 13. NOESY spectrum of pinofuranoxin B (**2**) ($CDCl_3$, 400 MHz).

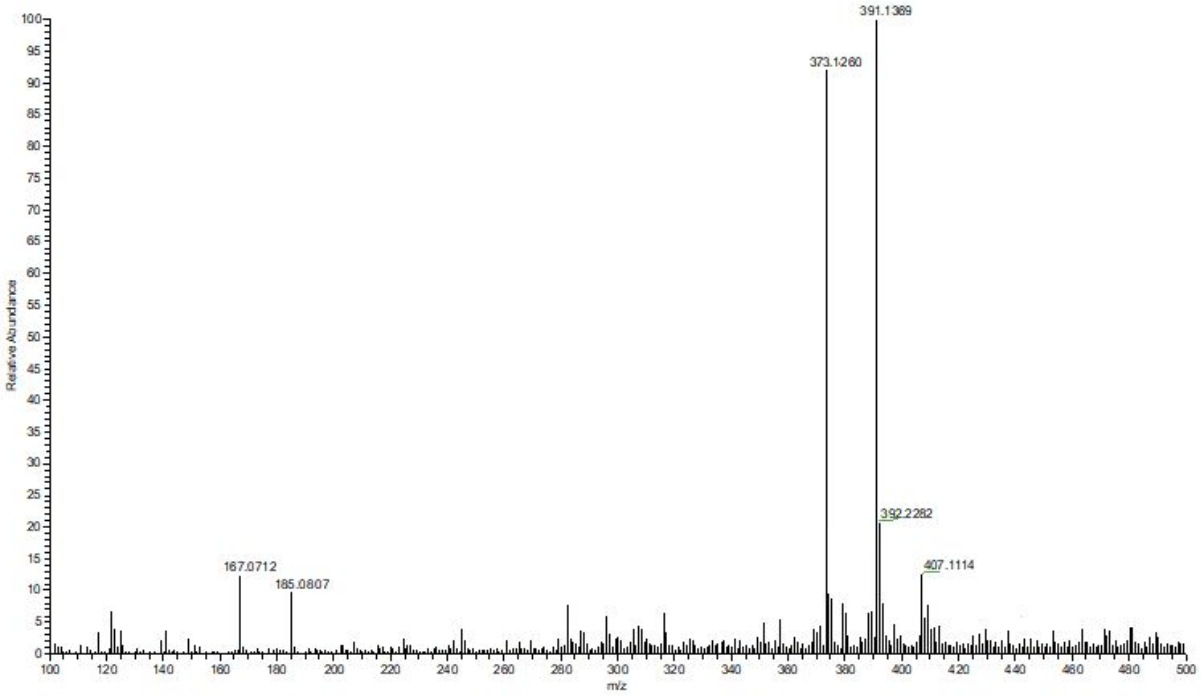

Spectrum 14. HR ESIMS spectrum of pinofuranoxin B (**2**).